ICAS 2021 SHANG HAI
International Council of the Aeronautical Sciences
32nd Congress of the International Council of the Aeronautical Sciences
September 6-10, 2021
Pudong Shangri-La, Shanghai, China

DESIGN OF A VERTICAL DITCHING TEST

G. Nicolosi[1], F. Valpiani[1], G. Grilli[1], A. Saponaro Piacente[1], L. Di Ianni,
E. Cestino[1], V. Sapienza[2], A Polla[1], P. Piana[3]

[1] Department of Mechanical and Aerospace Engineering, Polytechnic of Turin, Turin, Italy

[2] Aeronautical Engineering Consultant, Turin, Italy

[3] Tesco GO SRL, Chieri, Italy

Abstract

The current airworthiness regulation CS 23.527 describes the ditching of a seaplane. The regulation defines the pressure distribution along the structure profiles in line with the theoretical study carried out by T. Von Karman [1] and Wagner [2]. Therefore, the current rules describe the phenomenon without investigating the dynamic aspects of this phenomenon and the particular effects on the pressure/time relationship.
This research aims to investigate the behavior of the fluid-structure interaction during the specific impact phase. The objective is to study a methodology that can describe this phenomenon and thus allow the correct sizing of the seaplane hull during the impact on water. A step-by-step methodology based on numerical calculations using LS-DYNA and experimental ditching tests is proposed.

Keyword: Ditching Test, Fluid-Structure Interaction

1. Introduction

The study is carried out by the S55 student Team in collaboration with external engineering experts. TeamS55 is a team from polytechnic of Turin whose aim is to reproduce, in 1:8 scale, the s55 Savoia-Marchetti seaplane produced in Italy in the 1920s. To achieve this goal, historical models are studied and optimized through the knowledge and resources available nowadays [3] [4].
Particular attention is paid to the sizing of the hull, which is subject to phenomena of fluid-structure interaction generated during landing. In order to acquire the knowledge and skills necessary to optimize the hull, an experimental and numerical study on the behavior of a simplified wedge geometry is conducted.

To better understand the phenomenon, both analytical methods of T. Von Karman [1] and H. Wagner [2] and numerical study were used. For this study it has been used a multipurpose LS-DYNA software. With this software the user numerically replicates several physical phenomena. In particular it is possible to study the influence of the different variables involved, such as dihedral angle, impact velocity, and mass. The model used for this preliminary verification (Figure 1) include the adoption of the SPH (Smoothed Particle Hydrodynamics) methodology able to capture the normal pressures at water-body interface and other physical phenomena like the propagation of the sound wave within the fluid as shown in Figure 1 and 2.

A specific literature review was carried out in [2] [10] [12] to produce a versatile experimental setup for the preliminary study of wedge impact and future testing. The designed ditching structure was built in the laboratories of the Aerospace Department of the Polytechnic of Turin. The testing phase was carried out on a steel wedge instrumented with accelerometers and pressure sensors (*Figures 6 and 7*). The structure is able to release the test object from different heights to evaluate how the results change as the impact speed changes. A peculiarity of our study is the limited wedge weight of only 20.1 kg, which is much lower than other studies [9] [10] [11] based on wedges that exceed 100 kg.

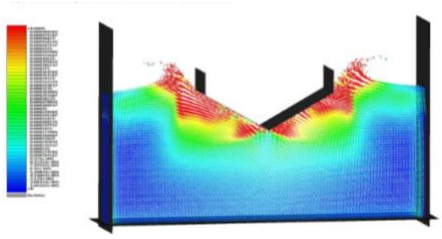

Figure 1 – Normal Pressure Interface, SPH Model

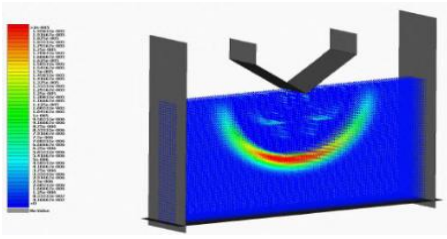

Figure 2 – Sound wave in fluid, SPH model

2. Experimental method

The process to design these experiments involved several phases. Firstly, it is necessary to define the test article and the ditching structure. In particular, the test article is the body on which runs the test and measures the desired phenomena. On the other hand, the ditching structure is the structure that allows the test article to execute the test under optimal conditions and controls.
In our case, the test article is a wedge, *Figure 3,* with a length of 950mm, a width of 254.81mm, and a dihedral angle of 30 degrees, *Figure 4.* The angle is the trade-off between higher values, which would drastically reduce the pressure measured, and lower values, which lead to the formation of air bubbles below the surface, which could modify the pressure measurement.

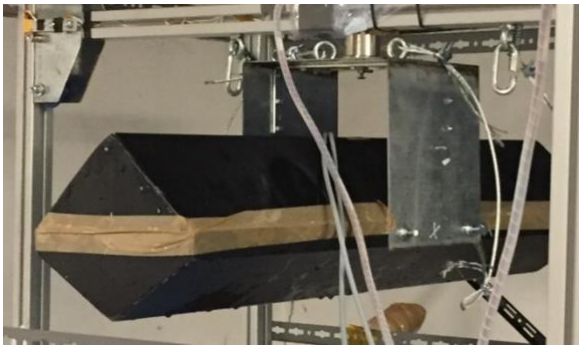

Figure 3 - The wedge system

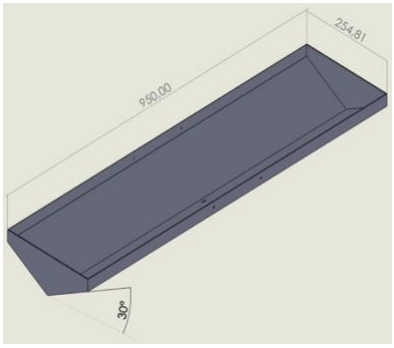

Figure 4 – The wedge dimensions

The wedge is composed of a single 2mm thick sheet of bent steel with welded side flanges. The production operations were carried out entirely within the laboratories of the Polytechnic of Turin. The wedge system weight is 20.1kg. Phenomena developed during the impact event are measured. The pressure sensors are mounted at the middle of the long side of the wedge, perpendicular to the wall: the lowest is 25mm from the apex and the second is 87.5mm from the apex (*Figure 5).* In order to correctly evaluate the pressure at impact, it was decided to place the sensor as close as possible to the vertex; the overall dimensions of the sensor and the support system set a physical limit of 25mm of distance from the vertex.

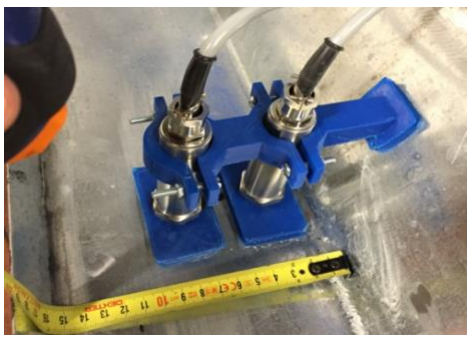

Figure 5 - Pressure sensor position

The sensors adopted are two HBM P3MB-050BRT pressure transducers, with a range of 50bar, called P1 and P2 as shown in *Figure 6.*
These transducers are located on the longitudinal plane fixed on the wedge's external surfaces. Moreover, there are the two Brüel & Kjær 4397A accelerometers with a range of 750g, called A1 and A2 as shown in Figure 6. The sensors have been selected to be used also in a subsequent vertical impact and ditching tests foreseen on the real 1:8 geometry of the S55 hull.

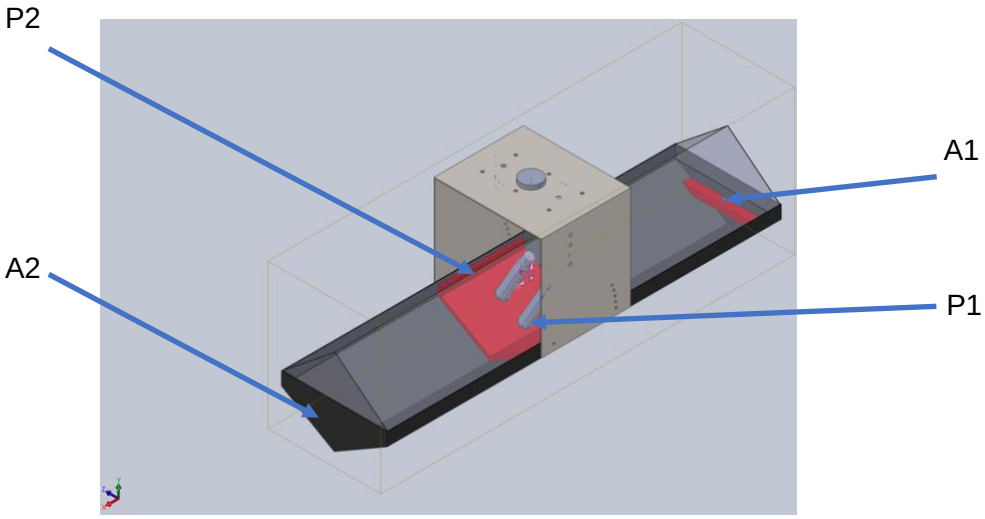

Figure 6 – Sensor definitions

The wedge system is completed with a with a triangular cover to set a perimetral enclosure constraint for the single plates, the transparent enclosure is visible at the top in *Figure 6.* The purpose of the enclosure is to prevent water from entering and damaging sensors and allowing the interface between the wedge and the ditching structure.

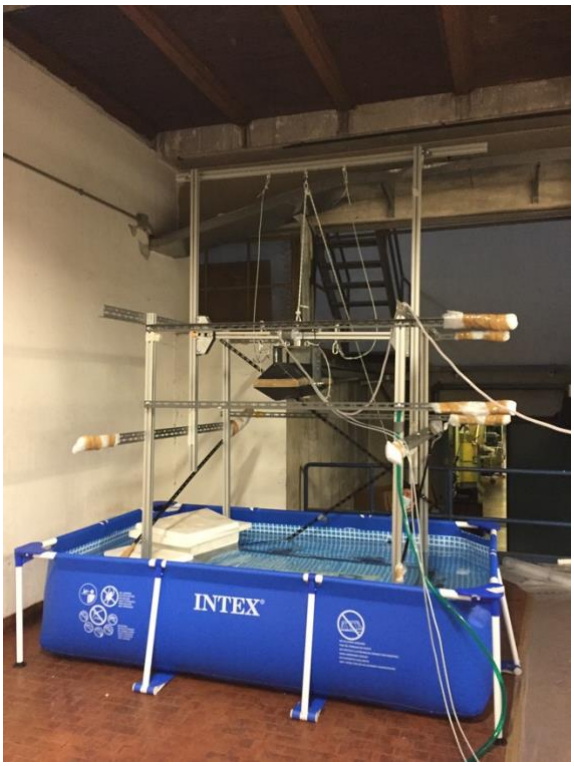

Figure 7 - The Ditching system with the wedge system installed.

Due to the space limitations of the lab, the maximum height available for the ditching system is 3m. Considering the dimensions of the wedge, the dimensions of the release system and the dimensions of the pool, the maximum fall height available is 1.70m. Table 1 shows the various test heights and corresponding impact speed.
The free-fall is the best solution to avoid kinetic energy losses due to friction between mechanical components, but its disadvantage is the impossibility of controlling the wedge kinetic at the impact. The rotation of the test article around its longitudinal y-axis (referring to the coordinate system in *Figure 9*) can reduce or increase the relative angle between the wedge plates and the calm water, this may affect the experimental results.

Cases	Height [m]	Speed [m/s]
1	0.40	2.80
2	0.60	3.43
3	0.70	3.70
4	0.80	3.96
5	1.00	4.43
6	1.20	4.85
7	1.30	5.05
8	1.50	5.42
9	1.70	5.77

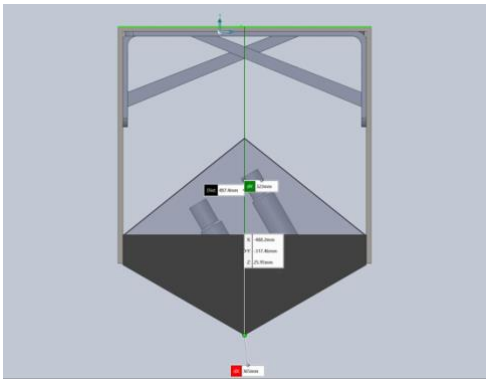

Table 1 – Test cases

During the experimentation, each test case is repeated three times.
The impact speed, showed in *Table 1,* has been calculated considering the conservation of energy principle:

$$mgh = \frac{1}{2}mV2 \qquad (1)$$

$$V = \sqrt{2hg} \qquad (2)$$

Where m is the wedge mass, $g = 9{,}81\ m/s^2$ is the acceleration of gravity, V is the impact speed.

4. Analytical Approach

Several analytical solutions that describe the water impact phenomenon are available in literature and always they introduced simplified geometric models. The specific formulation described below introduced simplified geometric models of a wedge that ditching the calm water.
In our case, we principally based our considerations on the theories of Von Karman [1] and Wagner [2], which are specifically based on the geometry of a rigid wedge. The main assumptions of these theories are based on the fact that the time period of the impact phenomenon is very short, and therefore it is possible to simplify the interaction process by neglecting the viscosity of water and the force of gravity, as demonstrated in the work of S. Abrate [5]. Moreover, the impact velocity is much lower than the speed of sound in the liquid, and for this reason, the fluid is considered incompressible.
Von Karman's formulation (1929) considers the maximum pressure at impact as a function of three main parameters: fluid density ρ, impact velocity v and dihedral angle α (defined as shown in *Figure 8)*:

$$P_{MAX} = \frac{1}{2}\rho v^2 \cdot \pi \cot \alpha \qquad (3)$$

The second theory used for comparison is the one developed by Wagner [2] in 1932. This theory considers the local uprise of water along the wedge surface, as shown in *Figure 8.* In this case, we

have a more refined model in which it is possible to evaluate the pressure peak as a function of position along the wedge length:

$$P(x) = \frac{1}{2}\rho v^2 \left[\frac{\pi}{tan\,\alpha \left(1 - \frac{x^2}{L^2}\right)^{\frac{1}{2}}} - \frac{\frac{x^2}{L^2}}{1 - \frac{x^2}{L^2}} + \frac{2\ddot{y}}{v^2}(L^2 - x^2)^{\frac{1}{2}} \right] \qquad (4)$$

where ρ Is the fluid density, v is the impact velocity, α is the dihedral angle in radian [13], L is the half-wetted breadth of the wedge measured horizontally and $\ddot{y}$ is the vertical acceleration. To evaluate the maximum pressure, it is necessary to derive the *Equation (4)* $\frac{dP(x)}{dx} = 0$ which gives:

$$P(\bar{x})_{MAX} = \frac{1}{2}\rho v^2 \left[1 + \frac{\pi^2}{4\,tan(\alpha^2)} \right] \qquad (5)$$

$$\bar{x} = L\left(1 - \frac{4\,tan^2\,\alpha}{\pi^2}\right) \qquad (6)$$

$\bar{x}$ is the coordinate of the maximum pressure measured with *Equation (5)*.
Equation (6) illustrates that the highest pressure is reached just before the end of the wetted region along the side of the wedge [2] due to water pile-up when the wedge penetrates the water. If the speed of the wedge is constant, the $\ddot{y}$ term would be null, and therefore the maximum pressure would be recorded towards the end of the oblique side of the wedge. Due to the impact, however, the sinking velocity is not constant, especially in case of light wedge (like the one characterized in these experiments): maximum pressure is expected at points adjacent to the vertex because the impact occurs earlier and therefore at a higher velocity.

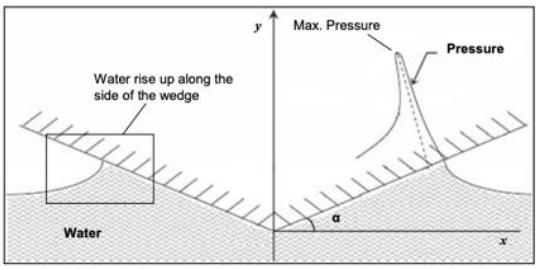

Figure 8 – Dihedral angle and half wetted breadth of the wedge [2]

5. LS-DYNA Simulation

LS-DYNA is a general-purpose dynamic finite element code capable of simulating complex real-world problems. LS-DYNA's strength is in the modeling of impact problems. An explicit time integration scheme is used to solve dynamic equations that characterize the different problems.
The purpose is to reconstruct the physical behavior of the impact with this general-purpose software.
In order to reduce the computational cost of the simulation, the problem could be reduced within its symmetry planes. For this purpose, the entire domain model could be realized by defining a simplified two-dimensional model. The details of this model, its characteristics, and its applicability will be described in following papers. An example of preliminary numerical study was conducted with the model presented in 2015 by NASA [6] about the impact of a sphere in water. The simulation is performed on a section of the actual case study to reduce the computational cost; symmetries of the problem have been used to carry out this simplified model.

4.1 Model

In *Figure 9* it is shown the comparison between the dimensions of the Simulated and the Experimental models. The experimental tank has to be extended along the X-axis to avoid the reflection of the wave produced by the lateral walls. Moreover, the wedge must have an adequate extension lengthwise along the y-axis to prevent edge phenomena that could affect the results.

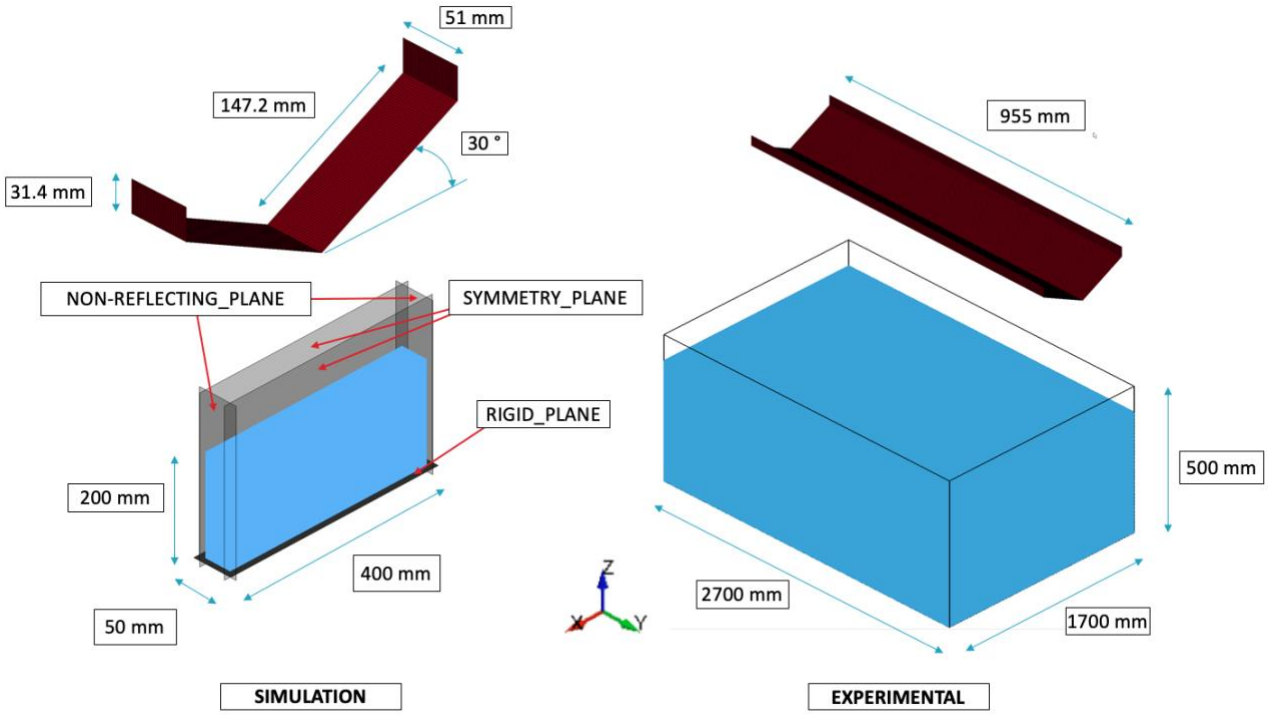

Figure 9 – Geometry comparison between the simulation model and experimental test

In the Simulated Model, four specific boundary conditions are used: two symmetry planes perpendicular to the Y-axis to mirror the behavior of the water inside the tank and two non-reflecting planes perpendicular to the X-axis that deactivate the reflection of the particles that hit them. The bottom of the simulated tank is made with a rigid plane, see the reference system in *Figure 9*. The smaller extension along the Z-axis is justifiable by observing the final image of the simulation shown in Figure 10. After a drop of about 40 millimeters in the water, the pressure developed in the bottom of the tank is negligible compared to those recorded on the wedge surface.

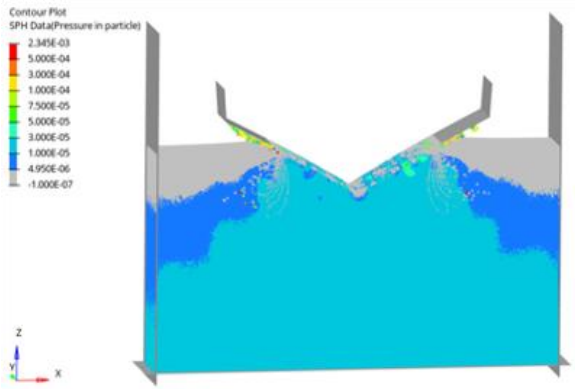

Figure 10 – Pressure developed after 40 millimeters drop

The wedge is modeled with simple shell elements defined by the Belytschko – Tsay formulation with at

least three integration points within a shell thickness of 2 millimeters. About the material property of the wedge, we used steel with the following properties: a density of $7.850E-06\ kg/mm^3$, Young's modulus of $210\ GPa$ and a Poisson's ratio of 0.3. The material is characterized as rigid; the only admitted DOF of the wedge is the rigid translation along the Z-axis. The real wedge has an empty structural mass of $5.59\ kg$: by adding instrumentation, it reaches a total mass of $W_r = 20\ kg$. Hence the wedge has about $14.4\ kg$ of non-structural mass. This mass can be attributed to the model using the MAREA (non-structural mass) parameter [7] ($S_r = 355414\ mm^2$), then the obtained result is applied to the area of the simulated model:

$$MAREA = \frac{W_r}{S_r} = 4.055E-05\ kg/mm^2$$

In conclusion, the simulated section of the wedge goes from an empty mass of $0.286\ kg$ to a total mass of $1.03\ kg$ and the initial kinetic energy is on a scale of about 1:20 with the kinetic energy of the real wedge.

4.2 Fluid Part

LS-DYNA implements different techniques to characterize the kinetic and fluid dynamic behavior of liquid material such as water.
The research developed here has focused on using and applying Smoothed Particle Hydrodynamics (SPH) elements. This procedure allows the definition of a Lagrangian mesh helpful in characterizing the behavior of components subject to considerable deformations and, for this reason, is suitable for the simulation of fluid-like or high-strain materials [7]. The SPH method secures the division of the liquid domain into a set of particles represented by different structural nodes inside the fluid domain. Each one of these particles can move freely and interact with each other or with other structures. Each particle/node defines a specific liquid volume, with a mass and an interaction volume. The water part is modeled by giving water material and through an Equation of State (EOS) that defines the behavior of the SPH particles [8].

4.3 Meshing and Computational Cost

The simulation involves the use of shell elements for the wedge and SPH elements for the fluid model. From interesting studies that will be published in future papers, it has been found that to obtain a good interaction between SHELL and SPH elements; it is necessary to have at least a mesh ratio lower than 2:1 between SHELL and SPH meshes. In our case, the geometry of the wedge is simple, so we used uniform QUAD elements with a 2mm edge. On the other hand, the water mesh has an SPH element for each millimeter. The request previously described between SHELL and SPH meshes strongly influences the computational cost. The model has 4 million SPH elements with about 4 thousand SHELL elements to respect the constraint of the 2:1 meshing ratio. The requested computing power was made available by the CASPER server of HPC@Polito.

4.4 Numerical Setup

The proposed tests aim to validate the experimental data acquired for three different impact velocities.: $5.05\ m/s$, $4.43\ m/s$, and $3.70\ m/s$ respectively. The end time of the analysis is set at 30 milliseconds: at the end, the wedge sinks inside the water by the quantities shown in *Figure 11.*
The principal analysis outputs are sensor 1 pressure, sensor 2 pressure, and impact deceleration. The pressure recorded is strongly dependent on the position of the measurement over the wedge faces: the elements considered as "sensors" in the simulation must be in the same position as the real sensors. In the following chapter, the numerical, experimental, and analytical results will be discussed and compared.

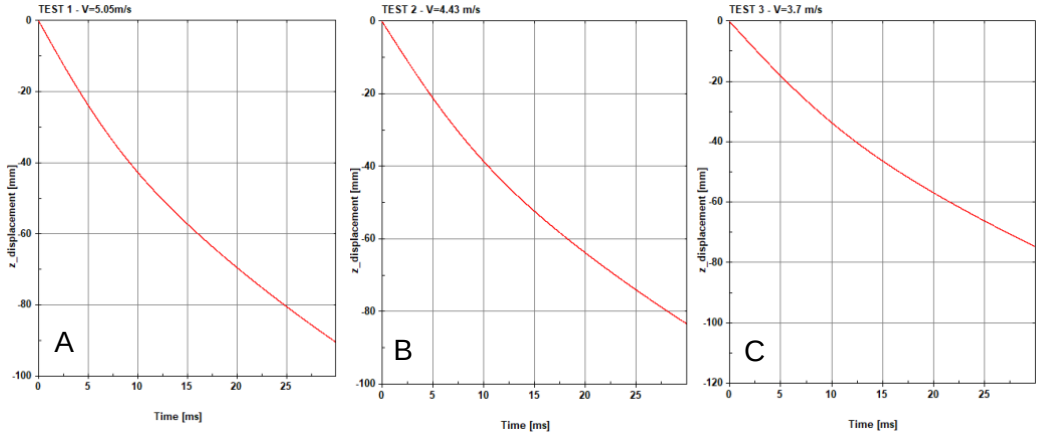

Figure 11 – Displacements of the wedge after 30 ms for the 3 Test cases: A) 5.05m/s, B) 4.43m/s, C) 3.70m/s

6. Results

6.1 Experimental Results

The duration of the phenomenon under consideration extinguish in approximately 10ms, as suggested by the numerical analyses presented in the previous chapter and as shown in other studies [10] [12]. In order to choose the correct sampling frequency, different frequencies available in the acquisition system were compared, and the results were evaluated. This comparison led to the exclusion of values below 2400Hz, for loss of information, and above 9600Hz, to avoid excessive noise and large data files. Based on the analysis reported and in line with the values typically used in similar studies, as shown by Lewis [12], 9600Hz was chosen as the sampling frequency.

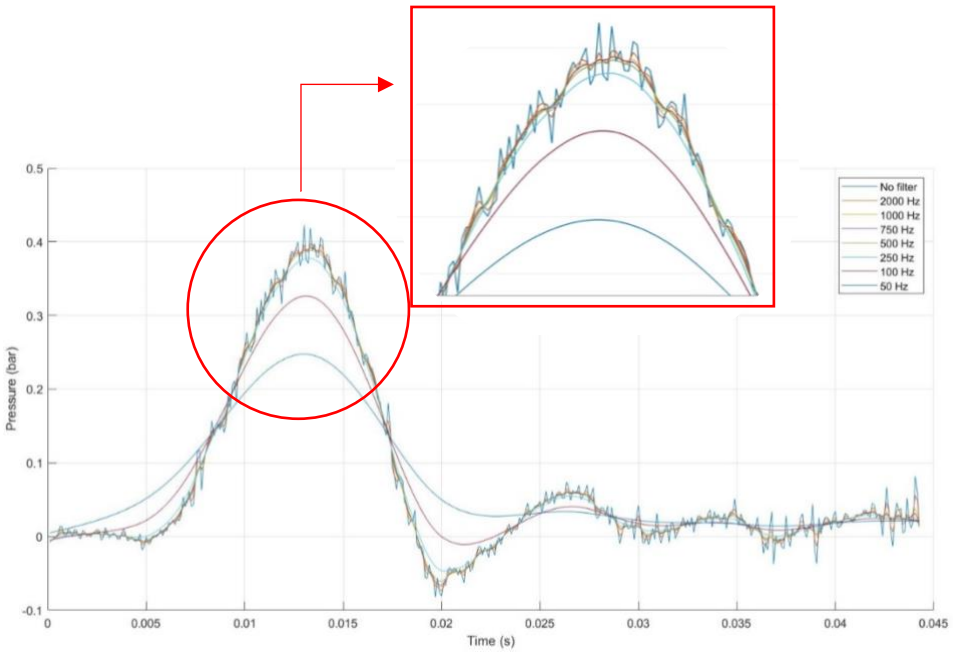

Figure 12 - Filter cut-off frequency comparison based on the ninth test case (h = 1.70 m)

Signals were filtered at 500Hz and 1200Hz with a low-pass Butterworth filter for pressure and acceleration respectively. These frequencies have been chosen by comparing different cut-off values and observing a lower limit that can avoid a significant reduction in the amplitude of the trend, as shown in Figure 12 for the pressure sensor. The superposition of the signal curves shows how much noise is cut by the Butterwort low-pass filter, as shown in *Figure 13* where the pressure and acceleration trends of the test with drop height 1.70m are shown. The figure below shows the filtered and unfiltered magnitudes in orange and blue, respectively.

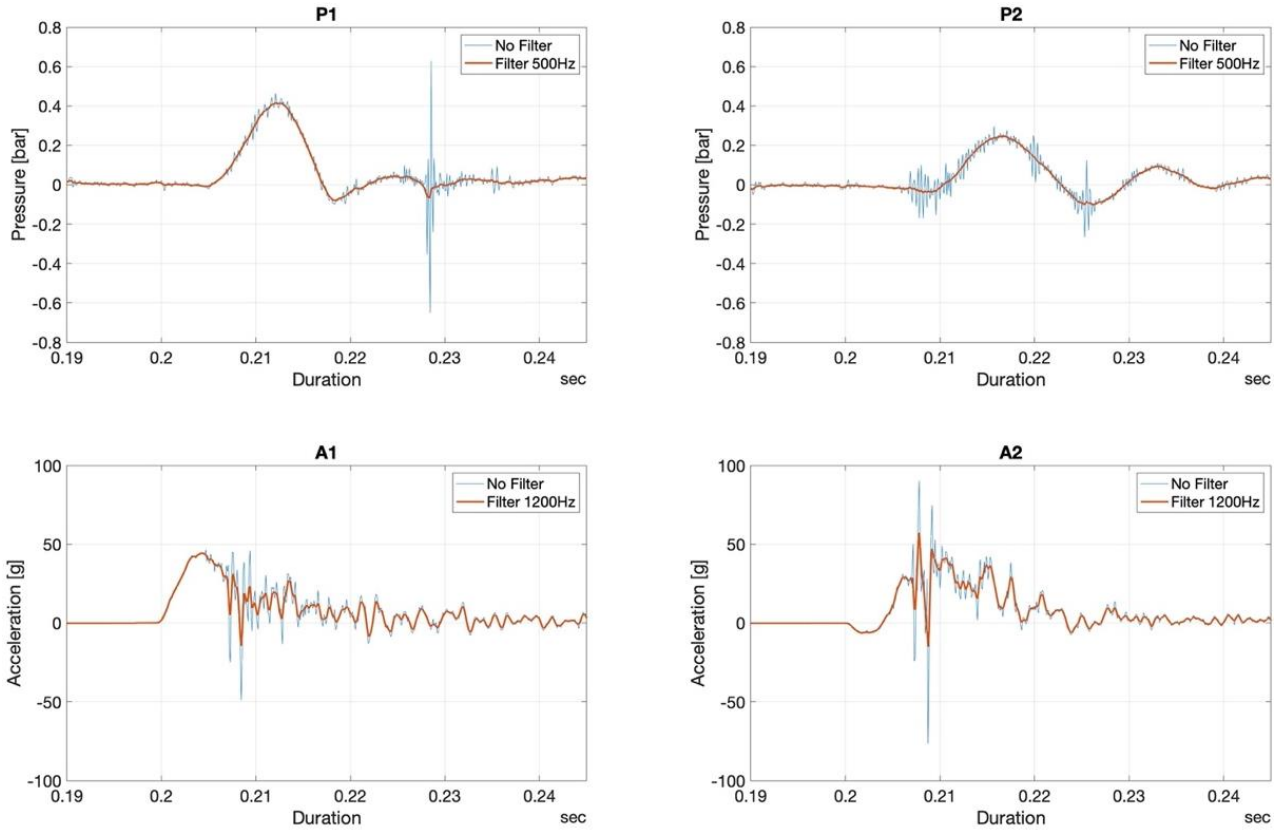

Figure 13 – Pressure and acceleration values measured at 1,70m release height

Figure 14 shows the comparison of values measured (P1 and P2) and the values calculated with the theory of Von Karman, yellow dots, and Wagner, blue dots. From the Figure 14 it can be seen that the experimental data are in good agreement with the theory of Von Karman below the height of 1m. Above, the differences seem more important, and several reasons could justify the differences. First of all, the values measured by the pressure sensors are close to the lower limit because the transducer range is very wide compared to the expected values. This may have generated a measurement error. Sensors were bought for a more complex test, in which the landing hull has a vertical and horizontal velocity component with the consequence of higher pressure. Another hypothesis concerns the wedge: in analytic theories, the test article is hypothesized to be infinitely rigid, while is not really true, so the deformation might have dissipated some impact energy.

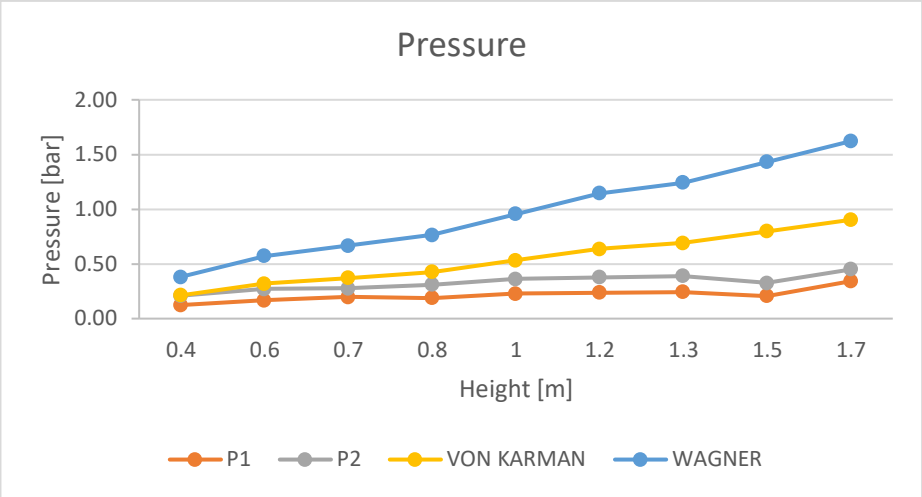

Figure 14 - Comparison of measured and numerical pressure calculated by Von Karman and Wagner theory.

As shown in *Figure 14*, the difference between the experimental and theoretical pressure is more significant at higher impact velocity. This might be explained by the wedge deformation due to the pressure developed. Furthermore, the rotation along the longitudinal wedge axes, due to an asymmetric distribution of weight, virtually changes the relative angle between the wedge plates and the calm water: as shown in *Figure 15* a slight rotation is captured by the support camera.

Figure 15 - Wedge impact instant for 1.70 m height test

The following graphs, *Figures 16, 17, and 18,* show the difference of pressure measured by the two sensors at three different heights: 0.40 m, 1.00m, and 1.70m. The orange curve is the P1 pressure sensor, and the blue curve is the P2 pressure sensor. The position of the sensors affects the measured pressure: the sensor P1 measures a higher value earlier in time than the sensor P2, which is located further from the wedge vertex. It is observed that, in contrast with what is expected from Wagner's theory, sensor 2 registers a lower pressure.
This effect is due to the weight of the wedge: having a very low weight, it undergoes a strong deceleration during the the test, which means that the impact of sensor 2 will be at a lower speed and therefore the pressure developed will be obviously lower.

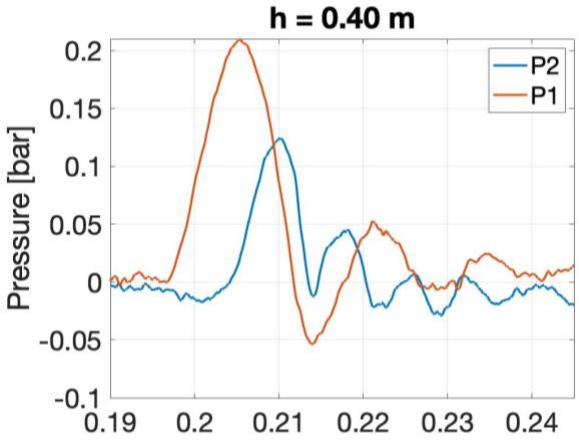

Figure 16 - Pressure - Test impact: h = 0.40 m

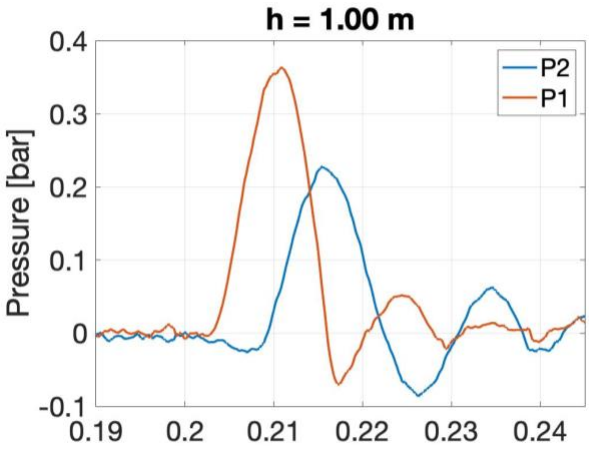

Figure 17 - Pressure - Test impact: h = 1.00 m

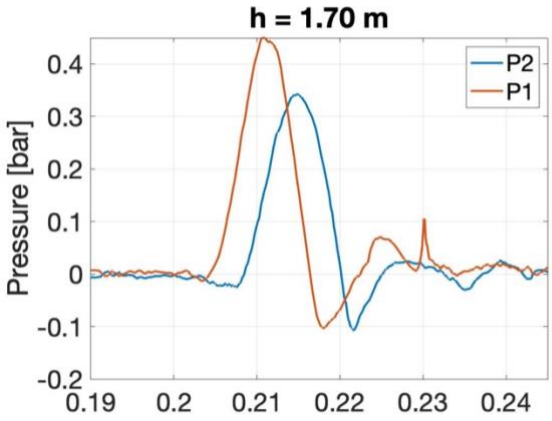

Figure 18 - Pressure - Test impact: h = 1.70 m

The following images show the data recorded by the accelerometers. *Figure 19* shows the peak of acceleration in each test; in *Figures 20, 21 and 22* displays the whole deceleration curve at impact for three different test.

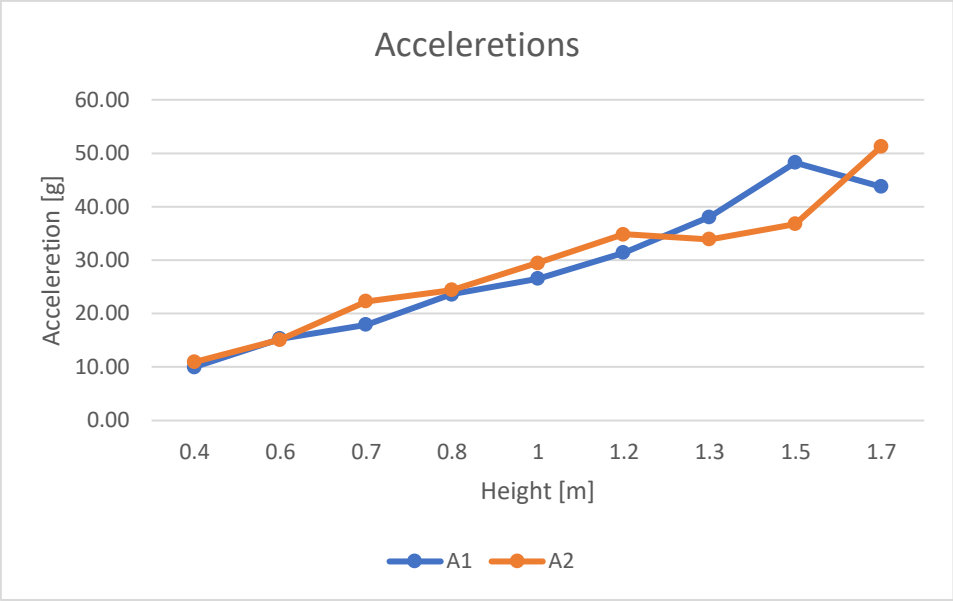

Figure 19 - Evolution of filtered acceleration and trend line

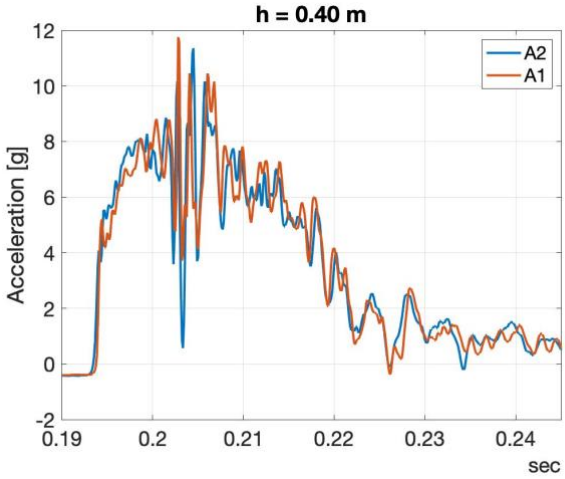

Figure 20 - Acceleration - Test impact: h = 0.40 m

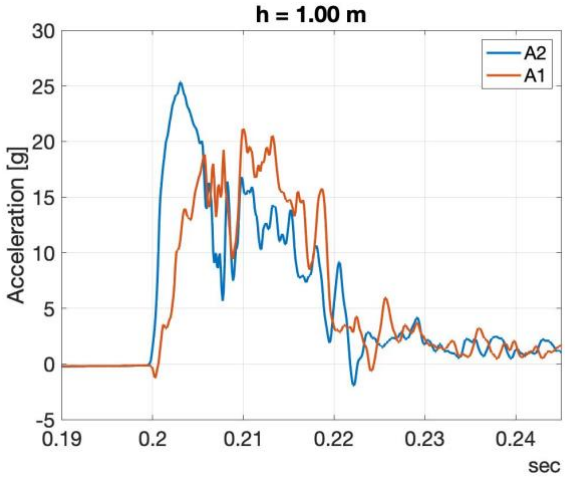

Figure 21 - Acceleration - Test impact: h = 1.00 m

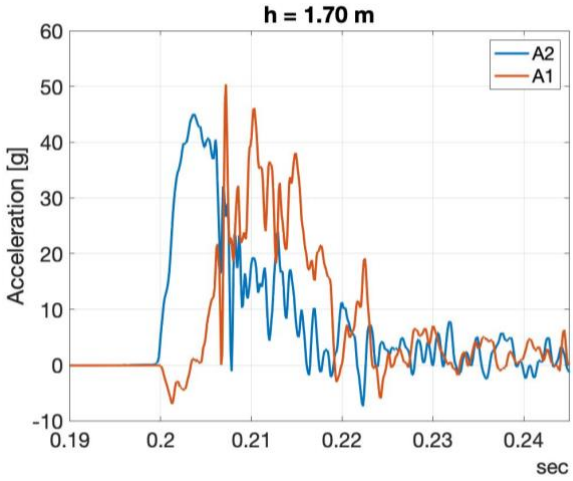

Figure 22 - Acceleretion - Test impact: h = 1.70 m

As shown in *Figures 20, 21 and 22*, as the height of the fall increases, it is observed a translation in time of one of the two curves that suggests a not completely horizontal impact of the wedge. A possible rotation around the x-axis (referring to the coordinate system shown in *Figure 9*) sometimes occurs during free fall: accelerations may be subject to error due to differential impact between the two extreme positions of the long side of the wedge. Moreover, similar to the pressure sensors, the range of the accelerometers is wider than necessary, this may cause some imprecision in the measurement. Another problem encountered is the unexpected liability of the constraints that hold the accelerometers in the correct position.

6.2 Numerical Results

LS-DYNA evaluates the pressure output on the area of the element [6]; a first data filter is performed by making an average of the pressures recorded by the 16 elements that are respectively in the positions of the first and the second real sensors, as shown in *Figure 23*. A second filter is applied for better reading: all presented curves have been filtered with a low-pass filter of 1kHz, as shown in the figure to reduce the characteristic contact noise of this type of numerical simulation *Figure 24.*

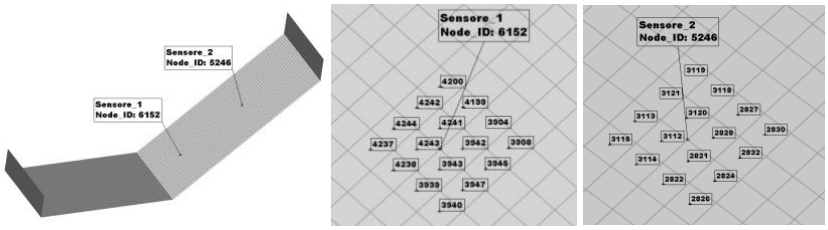

Figure 23 – A) Sensors positions, B) Elements of numerical pressure Sensor 1, C) Elements of numerical pressure Sensor 2

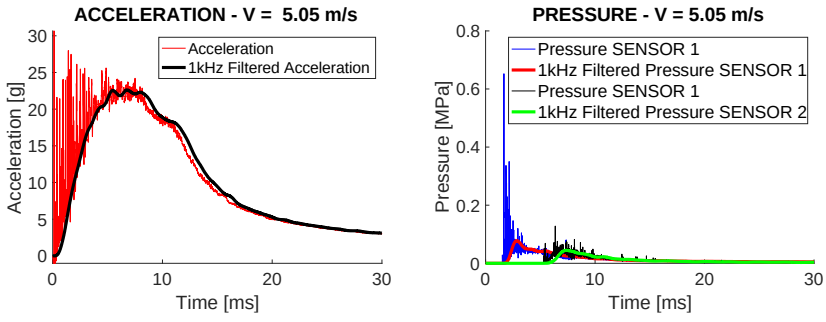

Figure 24 – Left, 1kHz filtered Acceleration Results for 5.05m/s impact velocity. Right, 1kHz filtered Pressure sensor 1 and sensor 2 results for 5.05m/s impact velocity

The following images show the numerical results of the three study tests. It is noticed that they have different scales for a better reading of the results of the single analysis:

- Test 01 – $V = 5.05\ m/s$

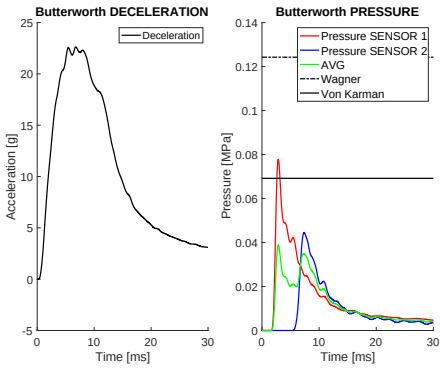

Max G Deceleration:	22.6 G
Pressure Sensor 1:	0.7783 bar
Pressure Sensor 2:	0.4458 bar
Von Karman's Theory:	0.6917 bar
Wagner's Theory:	1.2425 bar

Figure 23 – Numerical Results for 5.05m/s impact velocity

- Test 02 – $V = 4.43\ m/s$

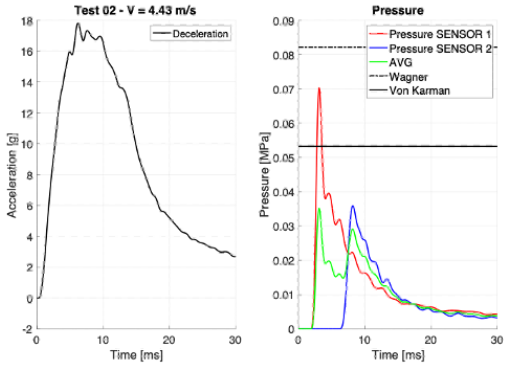

Max G Deceleration:	17.8 G
Pressure Sensor 1:	0.7027 bar
Pressure Sensor 2:	0.3589 bar
Von Karman's Theory:	0.5323 bar
Wagner's Theory:	0.9561 bar

Figure 24 – Numerical Results for 5.05m/s impact velocity

- Test 03 – $V = 3.70\ m/s$

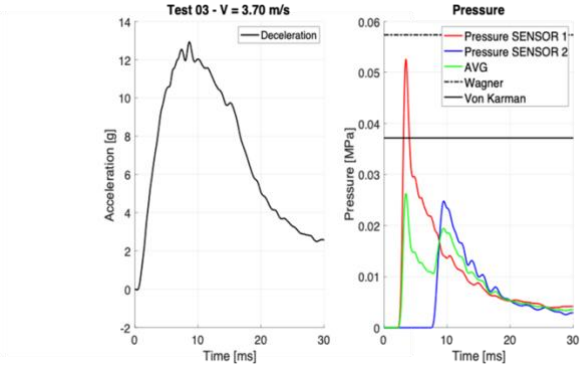

Max G Deceleration:	12.9 G
Pressure Sensor 1:	0.5253 bar
Pressure Sensor 2:	0.2478 bar
Von Karman's Theory:	0.3713 bar
Wagner's Theory:	0.6669 bar

Figure 25 – Numerical Results for 5.05m/s impact velocity

The maximum G-force is expected to be 22 G for the 5,05m/s impact velocity test (*Figure 23)* and the maximum pressure approximately 0.7 bar, as the sensor closest to the edge recorded and predicted. The figure below shows the pressure trend as a function of speed. By reducing the impact speed, the recorded pressures approach the value of Wagner's model while increasing the speed the pressure is closer to the value of Von Karman's model.

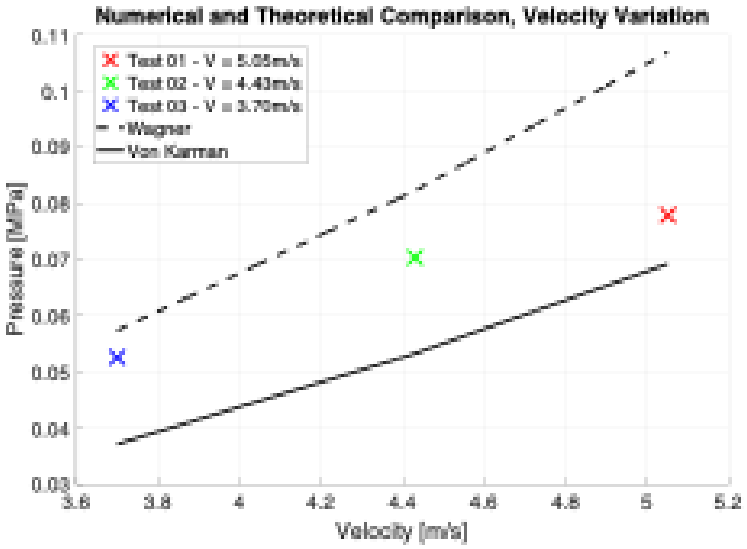

Figure 26 - Peak pressures recorded for the numerical tests compared with analytical theories

6.3 Numerical and experimental method comparison

The comparison in *Table 5* shows a difference in peak values for both pressures and accelerations between the data measured by the experimental test and those obtained from the numerical analyses. The experimental values displayed are calculated by averaging the values obtained for each of the three tests performed at different impact velocities. This difference is assumed to be due to inaccuracies in experimental data, as previously treated in the paragraph *"6.1 Experimental Results".*

Case	H	V	Experimental			Numerical			Analytic	
			Pressure		Acceleration	Pressure		Acceleration	Von Karman	Wagner
	m	m/s	bar		g	bar		g	bar	bar
			P1	P2	Max	S1	S2	MAX		
3	0,70	3,70	0,24	0,20	18,7	0,52	0,25	12,9	0,37	0,67
5	1,00	4,43	0,33	0,23	25,6	0,70	0,36	17,8	0,53	0,96
7	1,30	5,05	0,36	0,23	36,1	0,78	0.44	22,6	0,69	1,24

Table 5 - Comparison between the experimental and numerical results

On the other hand, the results of numerical simulations are in good agreement with the theories considered, as shown in Figure 26. It is observed that the pressure of sensor 2 (placed at a greater distance from the vertex of the wedge) is always lower than that of sensor 1. The phenomenon can be justified by the displacement profile shown in Figure 11. The velocity of the wedge progressively decreases upon impact, and sensor 2 will come to impact the water at a lower velocity than sensor 1 as it is further away from the vertex. In other studies [9][10][11], to eliminate this interaction, the weight of the wedge is increased so that the buoyancy-related decelerations are negligible. In our case, however, buoyancy must be considered with a view to future application on the complete hull of the S55 seaplane.

7. Conclusions

In this document, we described a method to design an experimental vertical ditching test and the comparison of its results with the numerical method. The results and considerations try to answer many questions raised during the design and the execution of different tests. As shown in *Table 5,* the different procedure results are similar in the numerical and analytical approaches but are different in the experimental procedure. This difference increases as the drop height increases due to a wedge flexibility effect and rotation of the expected impact configuration.

Results of the present study are a good starting point for a more complex investigation that will be made in the future in order to include the real hull geometry and flexibility effects. The test will be support with a more rigid structure that allow the wedge impact with the desired configuration.

Contact Author Email Address

The corresponding author can be contacted at the following email addresses: enrico.cestino@polito.it

Copyright Statement

8. Reference

[1] Karman V. The impact on seaplane floats during landing, NACA, 1929.
[2] Saha S.A. Water Impact Investigations for Aircraft Ditching Analysis thesis, School of Aerospace, RMIT University, 2010.
[3] Cestino E, Frulla G, Sapienza V, Pinto P, Rizzi F, Zaramella F, Banfi D. Replica 55 Project: A Wood Seaplane in The Era Of Composite Materials, *Proc of 31st ICAS Congress*, Belo Horizonte, Brazil, 2018.
[4] Favalli F, Ferrara M, Patuelli C, Polla A, Scarso S, Tomasello D. Replica 55 Project: Aerodynamic and FEM Analysis Of A Wooden Seaplane, *Proc of 31st ICAS Congress*, Belo Horizonte, Brazil, 2018.
[5] Abrate S. Hull Slamming, Department of Mechanical Engineering and Energy Processes, Southern Illinois University, 2014.
[6] Vassilakos G. J. Elemental Water Impact Test: Phase 1 20-inch Hemisphere, Analytical Mechanics Associates, Inc., Hampton, Virginia, NASA, 2015.
[7] LS-DYNA Keyword User's Manual, Volume I, Version R12, Livermore Software Technology Corporation, 2020.
[8] LS-DYNA Keyword User's Manual, Volume II, Version R12, Livermore Software Technology Corporation, 2020.
[9] Yettou El-M, Desrochers A, Champoux Y. A new analytical model for pressure estimation of symmetrical water impact of a rigid wedge at variable velocities, *Journal of fluids and structures*, Vol. 23, No. 3, pp 501-522, 2007.
[10] Yettou El-M, Desrochers A, Champoux Y. Experimental study on the water impact of asymmetrical wedge, *Fluid Dynamics Research*, Vol. 38, No. 1, pp 47, 2006.
[11] Dong C, Sun S, Song H, Wang Q. Numerical and experimental study on the impact between a free-falling wedge and water, *International Journal of Naval Architecture and Ocean Engineering*, Vol. 11, No. 1, pp 233-243, 2019.
[12] Lewis Simon G et al. Impact of a free-falling wedge with water: synchronized visualization, pressure and acceleration measurements, *Fluid Dynamics Research*, Vol. 42, No. 3, 2010.
[13] Chuang S-L. Slamming of rigid wedge-shaped bodies with various deadrise angles, Department of Navy, David Taylor Model Basin, Washington, D.C.